

# UC Davis

## IDAV Publications

### Title

Automatic Generation of Unstructured Grids for Volume Outside or Inside Closed Surfaces

### Permalink

<https://escholarship.org/uc/item/4zt9f4t9>

### Authors

Hamann, Bernd  
Chen, Jiann-Liang  
Hong, G.

### Publication Date

1994

Peer reviewed

Automatic generation of unstructured volume  
grids inside or outside closed surfaces

Bernd HAMANN<sup>1</sup>, Jiann-Liang CHEN<sup>2</sup> and Guangzhi HONG<sup>3</sup>

**Summary** - A new technique for unstructured volume grid generation around closed surfaces is presented. The technique is based on iterative point insertion. Grid point density depends on distance to the surface and surface curvature. The technique is completely automatic.

### 1. Introduction

An unstructured grid of a finite volume consists of a set of tetrahedra. Unstructured grid generation techniques can be automated to a high degree and typically require little user input, which is one of the most important advantages of unstructured grid generation over structured grid generation. In addition, unstructured grids are used more frequently now than a decade ago (see [10]).

There are two basic unstructured grid generation methodologies. The first one is based on the *advancing front* technique (see [8] and [9]), and the second one is based on the *Delaunay triangulation* of point sets (see [1], [2], [5], [6], [7], and [11]).

The technique introduced in this paper controls grid point density by considering distance to the surface and surface curvature. An initial volume grid with nearly constant grid point density is generated by intersecting line segments with the given geometry. The line segments are edges of a Delaunay triangulation of a sufficiently large box that completely contains the given geometry. The initial volume triangulation is iteratively modified by inserting points until a desired point distribution is obtained. In a preprocessing step, the method usually requires the reduction of the given surface triangulation (see [4]) and the approximation of absolute curvature at all points in the reduced surface triangulation (see [3]).

---

<sup>1</sup> Assistant Professor of Computer Science, NSF Engineering Research Center for Computational Field Simulation/Dept. of Computer Science, Mississippi State University, P.O. Box 6176, Mississippi State, MS 39762, U.S.A., hamann@erc.msstate.edu

<sup>2</sup> Ph.D. Student of Electrical and Computer Engineering, Department of Electrical and Computer Engineering, Mississippi State University, P.O. Drawer EE, Mississippi State, MS 39762, U.S.A.

<sup>3</sup> M.S. Student of Electrical and Computer Engineering, Department of Electrical and Computer Engineering, Mississippi State University, P.O. Drawer EE, Mississippi State, MS 39762, U.S.A.

It is assumed that a closed surface triangulation is given. Thus, each 3D point can be characterized as an exterior, interior, or point on the surface. It is possible to create an unstructured volume grid on the outside or the inside of the given surface. The algorithm requires these steps:

- (i) Compute a first volume triangulation for a 3D region that contains the given geometry.
- (ii) Intersect edges of volume triangulation with the surface.
- (iii) Characterize each vertex in the volume triangulation as an exterior point ("1"), point on the surface ("0"), or interior point ("1").
- (iv) Compute a second volume triangulation for the part lying inside (or outside) the closed surface.
- (v) Weight each tetrahedron according to surface distance and curvature of closest surface point.
- (vi) Insert additional grid points and locally update/improve the new volume triangulation.

## 2. Constructing the initial volume triangulation

The bounding box containing the closed surface is denoted by  $\mathcal{V}$ . The bounding box is scaled with respect to its centroid in order to define a sufficiently large space for the grid generation step. The surface itself is given by a set of points  $\mathcal{P} = \{x_i = (x_i, y_i, z_i) | i = 1, \dots, n\}$ , and an associated surface triangulation, denoted by  $\mathcal{T} = \{(v_1^j, v_2^j, v_3^j) | j = 1, \dots, m\}$ , where a triple  $(v_1^j, v_2^j, v_3^j)$  refers to three points in  $\mathcal{P}$  defining a triangle. A parametric surface representation might or might not be given.

Denoting the vertices of the (scaled) bounding box by  $b_{I,J,K} = (X_I, Y_J, Z_K)$ ,  $I, J, K \in \{0, 1\}$ , the hexahedron defined by these eight vertices is discretized by the points

$$y_{i,j,k} = \sum_{I,J,K \in \{0,1\}} b_{I,J,K} B_I^1(u_i) B_J^1(v_j) B_K^1(w_k), \quad (2.1)$$

where  $B_0^1(t) = (1 - t)$ ,  $B_1^1(t) = t$ ,  $t \in [0, 1]$ , and  $u_i$ ,  $v_j$ , and  $w_k$  are uniformly distributed parameter values in the interval  $[0, 1]$ . Each cuboid defined by eight vertices  $y_{i+r,j+s,k+t}$ ,  $r, s, t \in \{0, 1\}$ , is split into six tetrahedra. Thus, an initial volume triangulation is defined.

Each edge in this initial volume triangulation is intersected with the closed surface triangulation  $\mathcal{T}$ . Each point  $y_{i,j,k}$  can be characterized as lying outside the surface ("1"), inside a surface triangle ("0"), or inside the surface ("1"). This characterization is necessary in order to construct a volume triangulation for the outside (or inside) of the surface. In the following, the discussion is restricted to the generation of grids on the inside. If one needs to construct a grid on the outside, one must exchange the words inside and outside.

Tetrahedra can lie entirely on the outside of the surface, entirely on the inside, or lie partially on the outside and partially on the inside. The part of the initial volume triangulation that lies inside the closed surface must be extracted. Vertex indicators "-1," "0," and "1" are computed for each vertex of each tetrahedron in the initial volume triangulation. They are used to determine whether an edge  $\overline{v_i v_j}$  of a tetrahedron has an intersection point  $p_{i,j}$  with the given surface. Fourteen cases must be considered, assuming that an edge intersects a surface triangle in at most one point. Special care is required when an edge has more than one intersection. Tab. 1 lists all fourteen cases.

Case	Vertex indicators				Intersection point possible					
	$v_1$	$v_2$	$v_3$	$v_4$	$p_{1,2}$	$p_{1,3}$	$p_{1,4}$	$p_{2,3}$	$p_{2,4}$	$p_{3,4}$
1	-1	-1	-1	-1	n	n	n	n	n	n
2	0	-1	-1	-1	n	n	n	n	n	n
3	0	0	-1	-1	n	n	n	n	n	n
4	0	0	0	-1	n	n	n	n	n	n
5	0	0	0	0	n	n	n	n	n	n
6	1	-1	-1	-1	y	y	y	n	n	n
7	1	0	-1	-1	n	y	y	n	n	n
8	1	0	0	-1	n	n	y	n	n	n
9	1	0	0	0	n	n	n	n	n	n
10	1	1	-1	-1	n	y	y	y	y	n
11	1	1	0	-1	n	n	y	n	y	n
12	1	1	1	-1	n	n	y	n	y	y
13	1	1	1	0	n	n	n	n	n	n
14	1	1	1	1	n	n	n	n	n	n

Tab. 1: Indicators and possible intersections for single tetrahedron ( $p_{i,j} = y/n$  : edge  $\overline{v_i v_j}$  does/does not intersect surface in point  $p_{i,j}$ ).

Three of these fourteen cases are illustrated in Fig. 1. Circles indicate exterior points, stars indicate points in a surface triangle, and boldface points indicate interior points.

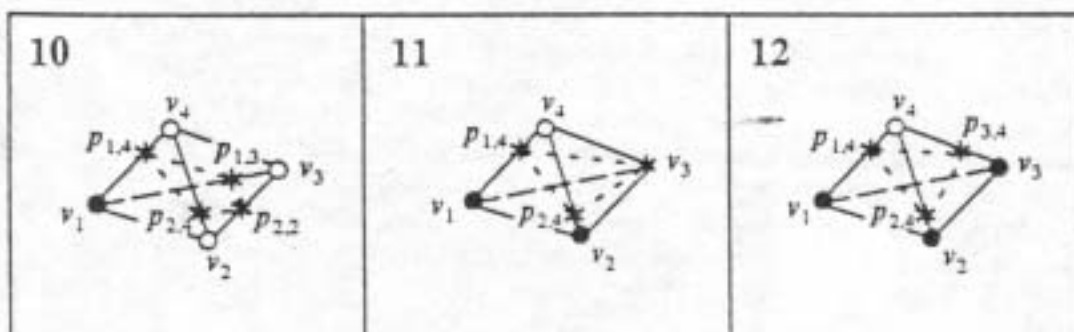


Fig. 1: Vertex indicators and intersection point.

Possible volume triangulations for the part of a tetrahedron that lies on the inside of the surface are listed in Tab. 2.

Case	First tetrahedron	Second tetrahedron	Third tetrahedron
1-4	-	-	-
5	$(v_1, v_2, v_3, v_4)$	-	-
6	$(v_1, p_{1,2}, p_{1,3}, p_{1,4})$	-	-
7	$(v_1, v_2, p_{1,3}, p_{1,4})$	-	-
8	$(v_1, v_2, v_3, p_{1,4})$	-	-
9	$(v_1, v_2, v_3, v_4)$	-	-
10a	$(v_1, v_2, p_{1,3}, p_{1,4})$	$(v_2, p_{1,3}, p_{1,4}, p_{2,4})$	$(v_2, p_{1,3}, p_{2,3}, p_{2,4})$
10b	$(v_1, v_2, p_{1,3}, p_{2,4})$	$(v_1, p_{1,3}, p_{1,4}, p_{2,4})$	$(v_2, p_{1,3}, p_{2,3}, p_{2,4})$
10c	$(v_1, v_2, p_{1,4}, p_{2,3})$	$(v_1, p_{1,3}, p_{1,4}, p_{2,3})$	$(v_2, p_{1,4}, p_{2,3}, p_{2,4})$
10d	$(v_1, v_2, p_{2,3}, p_{2,4})$	$(v_1, p_{1,3}, p_{1,4}, p_{2,4})$	$(v_1, p_{1,3}, p_{2,3}, p_{2,4})$
11a	$(v_1, v_2, v_3, p_{1,4})$	$(v_2, v_3, p_{1,4}, p_{2,4})$	-
11b	$(v_1, v_2, v_3, p_{2,4})$	$(v_1, v_3, p_{1,4}, p_{2,4})$	-
12a	$(v_1, v_2, v_3, p_{1,4})$	$(v_1, v_2, p_3, p_{3,4})$	$(v_2, p_{1,4}, p_{2,4}, p_{3,4})$
12b	$(v_1, v_2, v_3, p_{1,4})$	$(v_2, v_3, p_{1,4}, p_{2,4})$	$(v_3, p_{1,4}, p_{2,4}, p_{3,4})$
12c	$(v_1, v_2, v_3, p_{1,4})$	$(v_2, v_3, p_{1,4}, p_{3,4})$	$(v_2, p_{1,4}, p_{2,4}, p_{3,4})$
12d	$(v_1, v_2, v_3, p_{2,4})$	$(v_1, v_3, p_{1,4}, p_{2,4})$	$(v_3, p_{1,4}, p_{2,4}, p_{3,4})$
12e	$(v_1, v_2, v_3, p_{2,4})$	$(v_1, v_3, p_{2,4}, p_{3,4})$	$(v_1, p_{1,4}, p_{2,4}, p_{3,4})$
12f	$(v_1, v_2, v_3, p_{3,4})$	$(v_1, v_2, p_{2,4}, p_{3,4})$	$(v_1, p_{1,4}, p_{2,4}, p_{3,4})$
13	$(v_1, v_2, v_3, v_4)$	-	-
14	$(v_1, v_2, v_3, v_4)$	-	-

Tab. 2: Possible volume triangulations for cases 1-14.

Two volume triangulations are not listed in Tab. 2. They result from case 12 (Tab. 1). These two triangulations are necessary for the truncated part of a tetrahedron with a prism topology. Both triangulations require an additional vertex. The centroid  $c$  of the six points  $v_1, v_2, v_3, v_{1,4}, v_{2,4}$ , and  $v_{3,4}$  is used as additional vertex. In order to ensure consistency, i.e., face-to-face matching among all tetrahedra, one must choose either the eight tetrahedra  $(v_1, v_2, v_3, c)$ ,  $(v_1, v_2, v_{1,4}, c)$ ,  $(v_1, v_3, v_{3,4}, c)$ ,  $(v_2, v_3, v_{2,4}, c)$ ,  $(v_1, v_{1,4}, v_{3,4}, c)$ ,  $(v_2, v_{1,4}, v_{2,4}, c)$ ,  $(v_3, v_{2,4}, v_{3,4}, c)$ , and  $(v_{1,4}, v_{2,4}, v_{3,4}, c)$ , yielding volume triangulation 12h, or the tetrahedra  $(v_1, v_2, v_3, c)$ ,  $(v_1, v_2, v_{2,4}, c)$ ,  $(v_1, v_3, v_{1,4}, c)$ ,  $(v_2, v_3, v_{3,4}, c)$ ,  $(v_1, v_{1,4}, v_{2,4}, c)$ ,  $(v_2, v_{2,4}, v_{3,4}, c)$ ,  $(v_3, v_{1,4}, v_{3,4}, c)$ , and  $(v_{1,4}, v_{2,4}, v_{3,4}, c)$ , yielding volume triangulation 12i.

If an edge in the initial volume triangulation has more than one intersection with the given surface (or if an edge lies partially/completely in a triangle of the surface triangulation), an edge-surface intersection test is necessary. This test makes use of the fact that the end points of an edge  $\overline{v_i v_j}$  having an even number of intersections with a closed polyhedron, which is the closed surface triangulation, are *both interior* or *both exterior* points. Tab. 3 shows how to adjust the vertex indicators in this case.

Case	Initial indicators		# of intersections between $v_i$ and $v_j$	New indicators for		Selected intersection between $v_i$ and $v_j$
	$v_i$	$v_j$		$v_i$	$v_j$	
1	-1	-1	any number	-1	-1	none
2	-1	0	any number	-1	-1	none
3a	-1	1	even number	-1	-1	none
3b	-1	1	odd number	-1	1	one closest to $v_i$
4	0	0	any number	1	1	none
5	0	1	any number	1	1	none
6	1	1	any number	1	1	none

Tab. 3: Adjusting indicators for multiple edge-surface intersections.

If an entire edge (or part of an edge) in the initial volume triangulation is contained in a triangle (or more than one), the end points of the intersection are computed, and the end points are assigned the appropriate indicators.

If a parametric surface representation is known for the given surface, each intersection point between edges in the initial volume triangulation and the surface triangulation is mapped onto the parametric surface. This is done by expressing an intersection point in a triangle in terms of barycentric coordinates, using these barycentric coordinates to obtain a parameter value, and computing the corresponding point on the surface.

### 3. Adapting the volume triangulation by point insertion

At this point, the point density is nearly uniform throughout the unstructured grid on the surface's inside. A strategy is introduced that allows an increase in the point density close to the surface. Each tetrahedron is weighted according to its volume and the distance  $d_i$  between its centroid and the surface. The tetrahedral volumes should decrease with increasing distance. This can be achieved by defining a function  $V(d_i)$  for the desired tetrahedral volume. This function is

$$V(d_i) = \left[ 1 - \left( \frac{d_i}{d_1} \right)^p \right] V_0 + \left( \frac{d_i}{d_1} \right)^p V_1, \quad (3.1)$$

$p \in \{ \dots, \frac{1}{4}, \frac{1}{3}, \frac{1}{2}, 1, 2, 3, \dots \}$ , where  $V_0$  and  $V_1$  are specified tetrahedral volumes at distance 0 and distance  $d_1 > 0$ . Obviously, the gradient of the point density depends on the exponent  $p$ . It is possible to have tetrahedral volumes increase in a linear fashion ( $p = 1$ ), general polynomial fashion ( $p = 2, 3, 4, \dots$ ), or root fashion ( $p = \dots, \frac{1}{4}, \frac{1}{3}, \frac{1}{2}$ ).

The distance  $d_i$  between tetrahedron  $T_i$  with vertices  $v_1^i, v_2^i, v_3^i$ , and  $v_4^i$  and the surface is defined as the smallest distance between the tetrahedron's centroid and the vertices in the surface triangulation, i.e.,

$$d_i = \min \left\{ \left\| \frac{1}{4} \sum_{j=1}^4 v_j^i - x_k \right\|, k = 1, \dots, n \right\}, \quad (3.2)$$

where " $\| \cdot \|$ " denotes the Euclidean norm. Equation (3.1) can be interpreted in the following way: If  $V_i$  is the volume of tetrahedron  $T_i$ , and  $T_i$

has a distance  $d_i$  to the surface,  $T_i$  should have a volume  $V(d_i)$ . Thus, the difference between actual volume  $V_i$  and desired volume  $V(d_i)$  is given by

$$E_i = |V_i - V(d_i)|. \quad (3.3)$$

The average difference of the set of all tetrahedra and the desired tetrahedral volumes is defined as

$$E_{\text{avg}} = \frac{1}{L} \sum_{i=1}^L E_i, \quad (3.4)$$

where  $L$  is the number of tetrahedra.

A tetrahedron  $T_j \in \{T_i | i = 1, \dots, L\}$  is identified such that splitting it results in the smallest possible value  $E_{\text{avg}}'$ . The new average difference is given by

$$E_{\text{avg}}' = \frac{1}{L+3} \sum_{i=1}^{L+3} E_i'. \quad (3.5)$$

Furthermore, the distance  $d_i$  of a tetrahedron can be weighted by the absolute curvature  $\kappa_i$  of the surface point closest to the tetrahedron's centroid. If the objective is to create relatively small tetrahedra in regions close to surface areas with high absolute curvature, the value

$$\omega_i = \frac{\kappa_{\text{max}} - \kappa_i}{\kappa_{\text{max}} - \kappa_{\text{min}}} + \frac{1}{10} \frac{\kappa_i - \kappa_{\text{min}}}{\kappa_{\text{max}} - \kappa_{\text{min}}} \in \left[ \frac{1}{10}, 1 \right] \quad (3.6)$$

can be used as a weight for  $d_i$ , provided that  $\kappa_{\text{min}} \neq \kappa_{\text{max}}$ . Here,  $\kappa_{\text{min}}$  is the minimum and  $\kappa_{\text{max}}$  the maximum absolute curvature, considering all surface points.

Special care is required when splitting tetrahedra having edges or faces that are not shared by other tetrahedra. Case distinctions are based on a tetrahedron's neighbors and the number of surface points among its vertices. The surface boundary and the outer boundary must still be represented accurately after splitting. The possible cases are listed in Tab. 4.

Case	Surface points	Configuration
1	$v_1$	-
2a	$v_1, v_2$	Another tetrahedron shares the edge $\overline{v_1 v_2}$ .
2b	$v_1, v_2$	No other tetrahedron shares the edge $\overline{v_1 v_2}$ .
3a	$v_1, v_2, v_3$	Another tetrahedron shares the face $(v_1, v_2, v_3)$ .
3b	$v_1, v_2, v_3$	No other tetrahedron shares the face $(v_1, v_2, v_3)$ .
4a	$v_1, v_2, v_3, v_4$	All four faces are shared by other tetrahedra.
4b	$v_1, v_2, v_3, v_4$	The three faces $(v_1, v_2, v_3)$ , $(v_1, v_2, v_4)$ , and $(v_1, v_3, v_4)$ are shared by other tetrahedra, $(v_2, v_3, v_4)$ is not shared.

4c	$v_1, v_2, v_3, v_4$	The two faces $(v_1, v_2, v_3)$ and $(v_1, v_2, v_4)$ are shared by other tetrahedra, $(v_1, v_3, v_4)$ and $(v_2, v_3, v_4)$ are not shared.
4d	$v_1, v_2, v_3, v_4$	The face $(v_1, v_2, v_3)$ is shared by another tetrahedron, the other three faces are not shared.
4e	$v_1, v_2, v_3, v_4$	No face is shared by another tetrahedron.

Tab. 4: configurations when splitting tetrahedra with surface vertices.

When splitting tetrahedra having surface points among their vertices, midpoints of edges and centroids of faces are mapped onto the surface, provided its parametric definition is known (see Section 2). Possible volume triangulations for three of the cases listed in Tab. 4 are shown in Fig. 2.

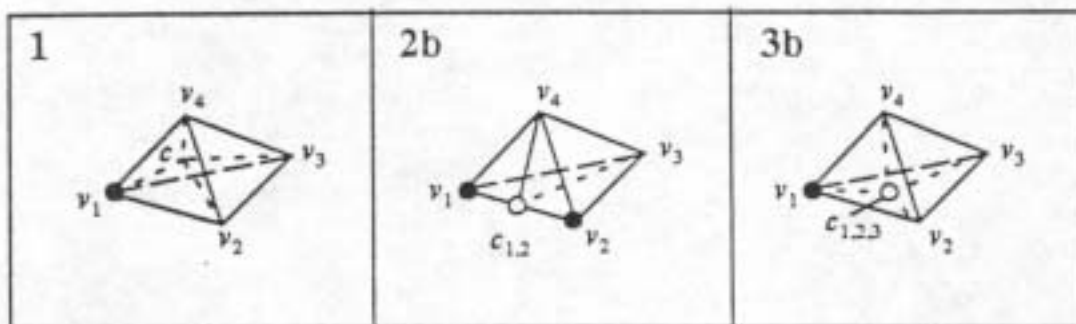


Fig. 2: Splitting tetrahedra having surface points as vertices.

#### 4. Improving the volume triangulation locally

In order to avoid tetrahedra that have small solid angles ( $S$ ) or small aspect ratios ( $D/A$ ) it is necessary to locally alter the volume triangulation. Considering a vertex  $v$  of a tetrahedron, the solid angle  $S$  at  $v$  measures the ratio of the surface area of the spherical triangle "cut out" by the edges and faces of the tetrahedron and the surface area of the associated sphere having  $v$  as its center. Here, the aspect ratio  $D/A$  of a tetrahedron is defined as the smallest distance  $D$  of any of the four vertex to an opposite face with area  $A$ . For most applications, a triangulation with fewer small solid angles/aspect ratios is a "better triangulation."

The volume triangulation is altered locally if this results in a better triangulation. A convex hexahedron  $\mathcal{CH}$  given by six triangular faces, nine edges, and five vertices can be triangulated in two ways. One can use either two or three tetrahedra. The alternative that maximizes the minimum solid angle is chosen. This is discussed in detail in [2], [6], and [7].

When splitting a tetrahedron  $T_i$ , the potential modifications of the volume triangulation are restricted to the neighbors of  $T_i$  and the tetrahedra replacing  $T_i$ . These are the steps of the local optimization procedure:

- (i) Determine the set  $\mathcal{O}_i$ , consisting of all neighbors of  $T_i$  and the tetrahedra replacing  $T_i$ .



- (ii) Perform steps (iii) and (iv) until the volume triangulation can not be improved any further.
- (iii) Find a convex hexahedron in  $\mathcal{O}_i$ ; for this hexahedron, select the triangulation that maximizes the minimum solid angle.
- (iv) Update  $\mathcal{O}_i$  if the volume triangulation has been altered.

This procedure might lead to a volume triangulation whose quality has decreased with respect to (3.1). Therefore, one should invoke the local optimization procedure only when the insertion of a point has created a solid angle that is smaller than some tolerance.

### 5. Examples

The method has been tested for parametrically defined closed surfaces (Fig. 3, Fig. 4, and Fig. 5) and for a closed surface triangulation without known parametric representation (Fig. 6). The surface triangulation without known parametric representation is an isosurface of a computerized axial tomography (CAT-scan) data set. In all four examples, grid points have been inserted by considering distance to the surface, but not considering surface curvature. The volume triangulations have been optimized locally by maximizing the minimum aspect ratio  $D/A$  after point insertion (see Section 4). The volume triangulations are intersected with cutting planes, and the intersections of the tetrahedra and the cutting planes (triangles and quadrilaterals) are shown. Certain tetrahedra have been made visible to illustrate their increasing/decreasing sizes.

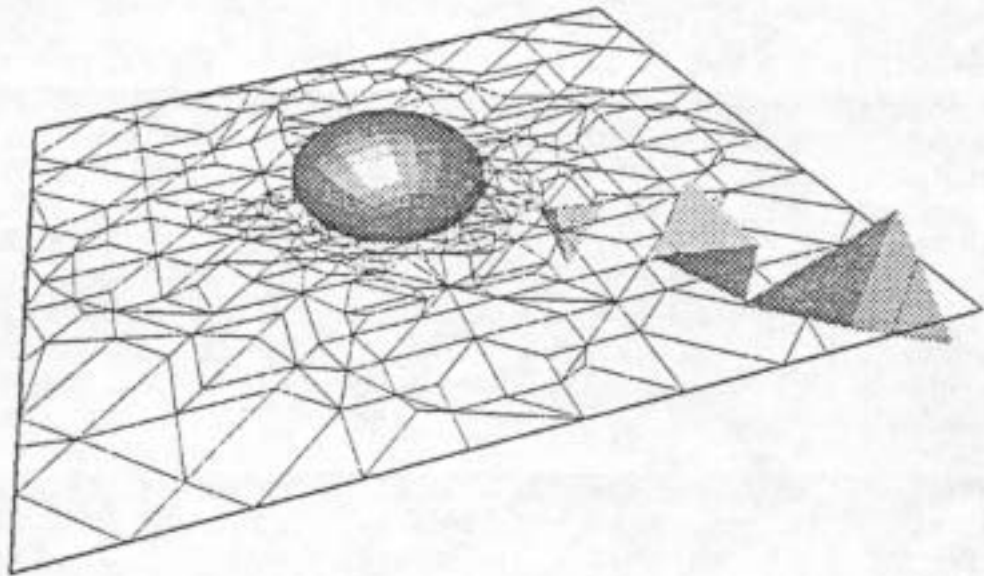


Fig. 3 : Unstructured grid around sphere.

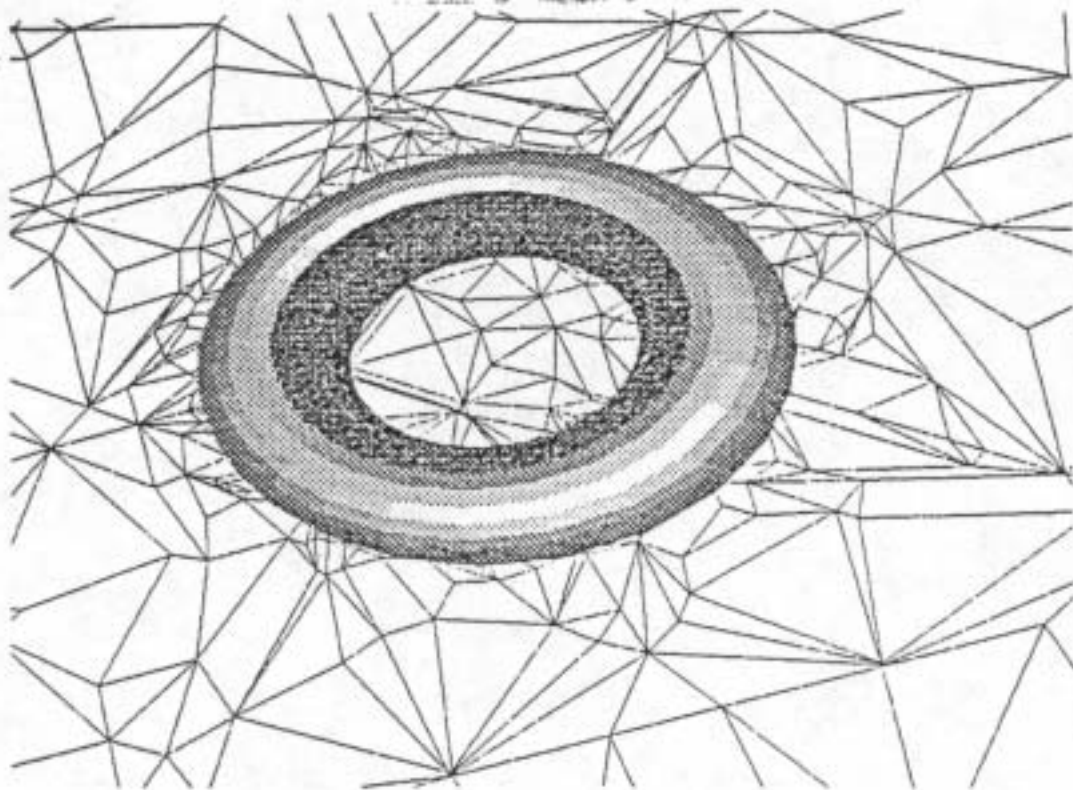


Fig. 4 : Unstructured grid around torus.

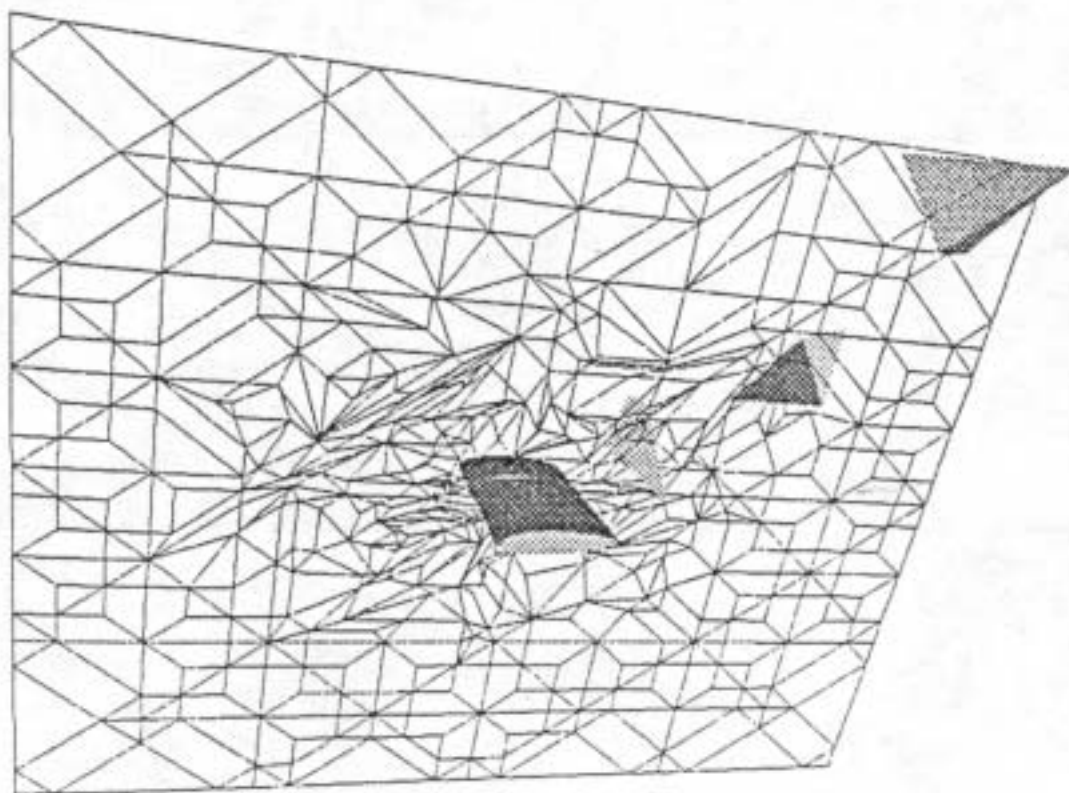


Fig. 5 : Unstructured grid around wing.

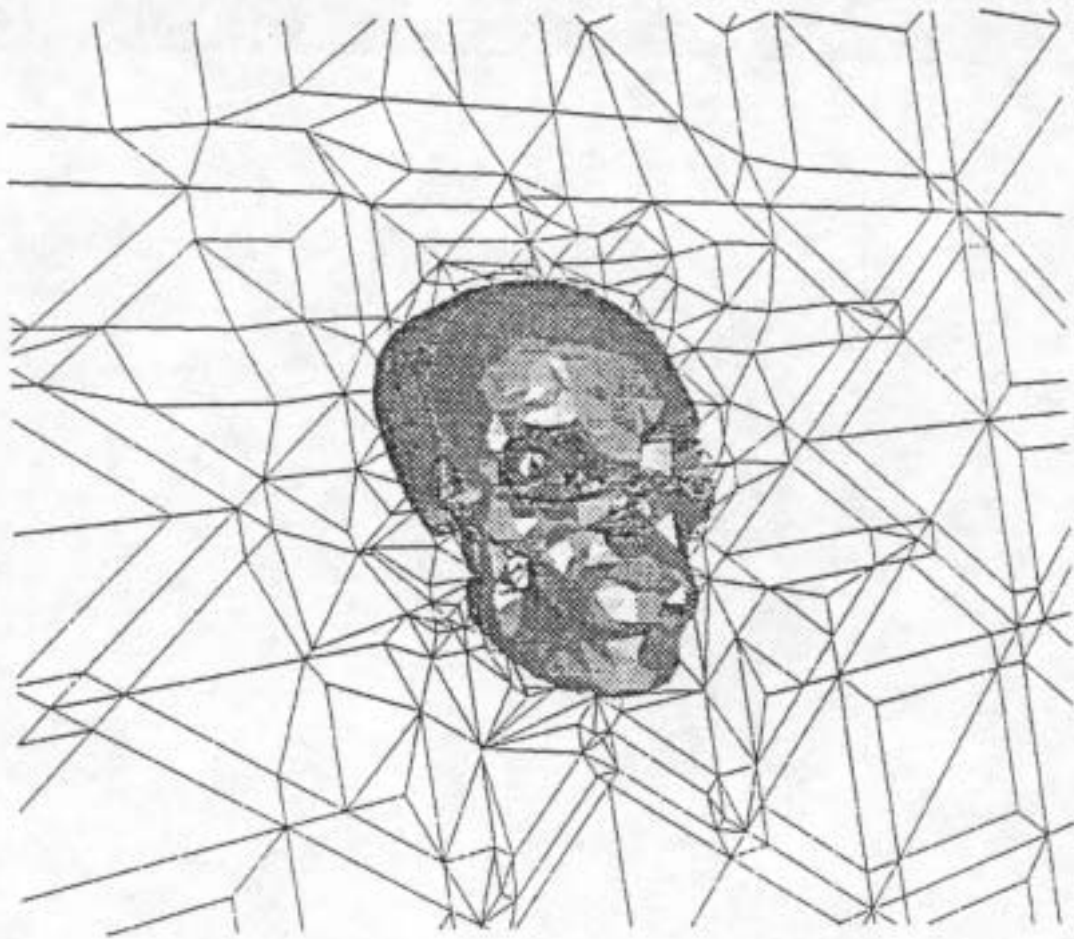


Fig. 6 : Unstructured grid around skull.

## 6. Conclusions

A completely automatic algorithm for constructing unstructured volume grids has been presented. The method is computationally fairly involved, but the test results confirm the validity of the approach. The fact that no user interaction is required for the grid generation process makes this method useful for complex closed geometries.

## 7. Acknowledgements

This work was supported by the National Science Foundation (Research Initiation Award 1992) under contract ASC-9210439 to Mississippi State University and by the National Grid Project consortium. Special thanks go to the members of the National Grid Project team at the NSF Engineering Research Center for Computational Field Simulation, in particular to Joe F. Thompson and Nigel P. Weatherill.

## REFERENCES

- [1] BAKER, T.J., Three-dimensional mesh generation by triangulation of arbitrary point sets, AIAA - 87 - 1124 - CP, pp. 255-271, 1987.
- [2] BARTH, T.J., WILTBERGER, N.L. and GANDHI, A.S., Three-dimensional unstructured grid generation via incremental insertion and local optimization, NASA - CP - 3143, pp. 449-461, 1992.
- [3] HAMANN, B., Curvature approximation for triangulated surfaces, in: Farin, G, Hagen, H. and Noltemeier, H., eds., Geometric Modelling, Springer-Verlag, New York, NY, pp. 139-153, 1993.
- [4] HAMANN, B., A data reduction scheme for triangulated surfaces, to appear in Computer Aided Geometric Design, Vol. 11, 1994.
- [5] HOLMES, G. and SNYDER, D., The generation of unstructured triangular meshes using Delaunay triangulation, in: Sengupta, S., Häuser, J., Eiseman, P.R. and Taylor, C., eds., Numerical Grid Generation in Computational Fluid Mechanics, Pineridge Press, Ltd., Swansea, U.K., pp. 643-652, 1988.
- [6] LAWSON, C.L., Software for  $C^1$  surface interpolation, in: Rice, J.R., ed., Mathematical Software III, Academic Press, San Diego, CA, pp. 161-194, 1977.
- [7] LAWSON, C.L., Properties of n-dimensional triangulations, Computer Aided Geometric Design, Vol. 3, pp. 231-246, 1986.
- [8] LÖHNER, R. and PARIKH, P., Three-dimensional grid generation by the advancing front method, International Journal for Numerical Methods in Fluids, Vol. 8, pp. 1135-1149, 1988.
- [9] PARIKH, P. and PIRZADEH, S., Recent advances in unstructured grid generation - Program VGRID3D, NASA - CP - 3143, pp. 435-448, 1992.
- [10] THOMPSON, J.F. and WEATHERILL, N.P., Aspects of numerical grid generation: Current science and art, Proceedings of the 11th AIAA Applied Aerodynamics Conference, Monterey, CA, August 1993.
- [11] WEATHERILL, N.P., A method for generating irregular computational grids in multiply connected planar domains, International Journal for Numerical Methods in Fluids, Vol. 8, pp. 181-197, 1988.